

# Constraints on millicharged dark matter and axion-like particles from timing of radio waves

Andrea Caputo,<sup>1</sup> Laura Sberna,<sup>2</sup> Miguel Frías,<sup>3</sup> Diego Blas,<sup>4</sup> Paolo Pani,<sup>5</sup> Lijing Shao,<sup>6</sup> and Wenming Yan<sup>7</sup>

<sup>1</sup>*Instituto de Física Corpuscular, Universidad de Valencia and CSIC,*

*Edificio Institutos Investigación, Catedrático Jose Beltrán 2, Paterna, 46980 Spain*

<sup>2</sup>*Perimeter Institute, 31 Caroline St N, Ontario, Canada*

<sup>3</sup>*Facultat de Física, Universitat de Barcelona, Martí Franquès 1, 08028 Barcelona, Catalonia, Spain*

<sup>4</sup>*Theoretical Particle Physics and Cosmology Group, Department of Physics,*

*King's College London, Strand, London WC2R 2LS, UK*

<sup>5</sup>*Dipartimento di Fisica, "Sapienza" Università di Roma & Sezione INFN Roma1, Piazzale Aldo Moro 5, 00185, Roma, Italy.*

<sup>6</sup>*Kavli Institute for Astronomy and Astrophysics, Peking University, Beijing 100871, China*

<sup>7</sup>*Xinjiang Astronomical Observatory, CAS, 150 Science 1-Street, Urumqi, Xinjiang, 830011, China*

We derive novel constraints on millicharged dark matter and ultralight axion-like particles (that may or may not be part of the dark matter sector) using pulsar timing and fast radio burst observations. Millicharged dark matter affects the dispersion measure of the time of arrival of radio pulses in a way analogous to free electrons. Light pseudo-scalar particles generically modify the dispersion measure in the presence of magnetic fields through the axial coupling. Furthermore, if they constitute the dark matter, they generate an oscillating polarization angle of the radio signals. We show that current and future data can set strong constraints in both cases. For dark matter particles of charge  $\epsilon e$ , these constraints are  $\epsilon/m_{\text{milli}} \lesssim 10^{-9} \text{eV}^{-1}$ , for masses  $m_{\text{milli}} \gtrsim 10^{-6} \text{eV}$ . The bound scales as  $(\rho_{\text{milli}}/\rho_{\text{dm}})^{1/2}$  if the millicharged component is a fraction of the total dark matter energy density,  $\rho_{\text{dm}}$ . For axion-like particles, we derive the expected bounds on the the axial coupling from modifications in the dispersion of the pulses in the presence of the observed galactic magnetic fields. We also bound this coupling from data of pulsar polarization in the case where (ultra-light) axion-like particles constitute the dark matter. Our analysis shows that the study of radio waves from pulsars can set the most stringent constraints on axion-like particles for  $m_a \sim 10^{-22}\text{--}10^{-15} \text{eV}$ .

Unraveling the nature of dark matter (DMa) is among the most urgent issues in fundamental physics. Indirect searches aim at detecting the effects of DMa in astrophysical observations, beyond its pure gravitational interaction. Given the feeble interaction of DMa with standard model fields, precise measurements are particularly promising for these searches. When one requires precision, a particular measurement stands out in astrophysics: the time of arrival of radio wave from pulsars and fast radio bursts (FRBs). The use of pulsar timing has already been suggested to study the effects of dark matter [1–9]. In this *Letter* we present new results for DMa models directly coupled to light from the propagation of radio pulses from pulsars and FRBs. A more comprehensive exploration will be presented elsewhere [10].

If DMa is coupled to the electromagnetic field, one expects modifications in the *emission*, *propagation*, and *detection* of radio pulses. We focus here on the effects during the propagation, which are robust under astrophysical uncertainties. In particular, we derive stringent constraints on millicharged DMa and axion-like particles (ALPs) based on a novel frequency dependence of the time of arrival (TOA) of radio signals from pulsars and FRBs, and on the modulation of the light polarization angle due to axion-like DMa in the Milky Way.

We give a unified treatment valid for both millicharged DMa and ALPs, considered as independent species. In the former case we consider that (a fraction of) the DMa is made of particles with mass  $m_{\text{milli}}$  and electric

charge  $q = \epsilon e$  ( $\epsilon \ll 1$ ) [11–17], whereas in the latter case we assume the existence of axion-like [18–20], pseudo-scalar particles, which may or may not be part of the DMa. The field equations read

$$(\square - m_a^2)\phi = -\frac{g}{4}F_{\mu\nu}\tilde{F}^{\mu\nu}, \quad (1)$$

$$\partial_\mu F^{\mu\nu} = 4\pi e j^\nu + 4\pi \epsilon e j_{\text{milli}}^\nu - \frac{g}{2}\epsilon^{\mu\rho\lambda\nu}F_{\mu\rho}\partial_\lambda\phi, \quad (2)$$

where  $g$  is the ALP-photon axial coupling,  $j^\nu$  is the ordinary electron current, whereas  $j_{\text{milli}}^\nu$  is the current from millicharged particles.

**Dispersion in the TOA.** We consider the propagation of a light signal of frequency  $\nu = \omega/(2\pi)$  along the  $z$  direction in the presence of a homogeneous background magnetic field polarized along (say) the  $y$  direction,  $\vec{B} = (0, B, 0)$ . For the first part of this work, DMa is considered as a cold-medium with vanishing background values for the fields appearing in (1)-(2). When  $\omega \gg m_a$ , propagation of the light signal in this medium is described by the first-order system  $i\frac{\partial}{\partial z}|\psi(z)\rangle = \mathcal{M}|\psi(z)\rangle$ , where the  $|\psi(z)\rangle$  is a linear combination of the two photon polarizations along the  $x$  and  $y$  directions and of the ALP state [21]. The  $3 \times 3$  mixing matrix reads [22]

$$\mathcal{M} := \begin{pmatrix} \omega + \Delta_{xx} & \Delta_{xy} & 0 \\ \Delta_{yx} & \omega + \Delta_{yy} & gB/2 \\ 0 & gB/2 & \omega - m_a^2/(2\omega) \end{pmatrix}. \quad (3)$$

The off-diagonal terms  $\Delta_{xy}$  and  $\Delta_{yx}$  give rise to Faraday rotation by mixing the photon polarizations and do not

play a role in this section. The diagonal terms  $\Delta_{xx}$  and  $\Delta_{yy}$  contain both QED vacuum polarization effects and plasma effects [21, 22]. The former ones are of order  $\Delta_{xx}^{\text{QED}} \sim \Delta_{yy}^{\text{QED}} \sim \omega \frac{e^2}{45\pi} \left(\frac{B}{B_c}\right)^2$ , where  $B_c = m_e^2/e \approx 4 \times 10^{13}$  G [23]. We shall only consider interstellar magnetic fields, for which  $B \ll B_c$  and  $\Delta^{\text{QED}}$  effects are negligible. Plasma effects arise from the presence of free charges. In the limit where the photon energy is much smaller than the mass of the charged, cold particles [24–26],

$$\Delta_{xx}^{\text{plasma}} \sim \Delta_{yy}^{\text{plasma}} \sim -\frac{\omega_p^2}{2\omega}, \quad (4)$$

where  $\omega_p^2 := \sum_i \frac{4\pi n_i q_i^2}{m_i}$  is the plasma frequency for particles with charge  $q_i$ , mass  $m_i$ , and number density  $n_i$ . The normal modes corresponding to (3) satisfy

$$k_0 = \omega - \frac{\omega_p^2}{2\omega}, \quad k_{\pm} = \frac{4\omega^2 - \omega_p^2 - m_a^2 \mp \sqrt{\Delta}}{4\omega}, \quad (5)$$

with

$$\Delta = \omega_p^4 - 2m_a^2\omega_p^2 + m_a^4 + 4B^2g^2\omega^2.$$

The TOA of a signal traveling at speed  $v = \partial\omega/\partial k$  across a distance  $d$  is  $T = \int_0^d \frac{dl}{v} = \int_0^d dl \frac{\partial k}{\partial \omega}$  along the line of sight. The previous expressions can be simplified by noticing that in most situations  $\omega_p \ll \omega$ . In this limit,

$$v_0^{-1} = 1 + \frac{\omega_p^2}{2\omega^2}, \quad (6)$$

$$v_{\pm}^{-1} = 1 + \frac{m_a^2 + \omega_p^2}{4\omega^2} \pm \frac{Y}{4\omega^2} (\omega_p^2(2 - Y^2) - m_a^2), \quad (7)$$

for the three polarizations, where we defined the dimensionless quantity  $Y := (1 + \eta^2)^{-1/2}$  with  $\eta := 2gB\omega/m_a^2$ .

In the absence of new physics ( $\epsilon = g = 0$ ), the two photon degrees of freedom propagate with  $k^2 = \omega^2 - \omega_p^2$ . For a photon with frequency  $\nu$ , a background of cold free electrons yields a time delay

$$\Delta t_{\text{DM}}^{\text{astro}} \sim 4.15 \left( \frac{\text{DM}_{\text{astro}}}{\text{pc cm}^{-3}} \right) \left( \frac{\nu}{\text{GHz}} \right)^{-2} \text{ ms}, \quad (8)$$

relative to a photon with infinite energy. Here  $\text{DM}_{\text{astro}} := \int n_e dl$  is the standard dispersion measure (DM) from electrons with number density  $n_e$  along the light of sight.

**TOA constraints on millicharged DMa.** We now focus on the case of millicharged DMa, i.e.  $g = 0$ . In this case the DM in (8) is dominated by the sum of the contributions from ordinary electrons and millicharged particles (see also [27]),  $\text{DM}_{\text{obs}} = \text{DM}_{\text{astro}} + \text{DM}_{\text{milli}}$ , where

$$\text{DM}_{\text{milli}} = \left( \frac{\epsilon}{m_{\text{milli}}} \right)^2 m_e \int dl \rho_{\text{milli}}, \quad (9)$$

where  $\rho_{\text{milli}}$  is the density of millicharged particles, which is equal to or smaller than the DMa density  $\rho_{\text{dm}}$ . While

the effect of  $\text{DM}_{\text{astro}}$  and  $\text{DM}_{\text{milli}}$  are completely degenerate, for a source at a distance  $d$  any measurement of the DM can be translated into a *conservative* upper bound on  $\epsilon/m_{\text{milli}}$  by simply requiring that all the DM is due to DMa, i.e.  $\text{DM}_{\text{milli}} < \text{DM}_{\text{obs}}$ . This yields

$$\frac{\epsilon}{m_{\text{milli}}} \lesssim \frac{10^{-8}}{\text{eV}} \sqrt{\frac{0.3 \text{ GeV/cm}^3}{\rho_{\text{milli}}}} \sqrt{\frac{\text{DM}_{\text{obs}}}{20 \text{ pc/cm}^3}} \sqrt{\frac{400 \text{ pc}}{d}}, \quad (10)$$

where we normalized the quantities by typical values within the galaxy. This estimate gives already a rather stringent bound, which can be refined through a Bayesian analysis. Given a theoretical hypothesis ( $\text{DM}_{\text{obs}} = \text{DM}_{\text{astro}} + \text{DM}_{\text{milli}}$ ), and a set of measurements of  $\text{DM}_{\text{obs}}$  from  $N$  pulsars, we construct the log-likelihood as

$$\ln \mathcal{L} = -\frac{1}{2} \sum_{i=1}^N \frac{(\text{DM}_{\text{obs}}^i - \text{DM}_{\text{astro}}^i - \text{DM}_{\text{milli}}^i)^2}{\sigma_i^2}. \quad (11)$$

Here  $\sigma_i$  is the dispersion for each pulsar, obtained adding in quadrature statistical uncertainties on  $\text{DM}_{\text{obs}}^i$  and the astrophysical ones on  $\text{DM}_{\text{astro}}^i$ . A similar technique was used in Ref. [28]. We used a uniform prior on  $\epsilon/m_{\text{milli}} > 0$  and verified that our results do not depend on this choice.

We shall consider a dataset of local pulsars and therefore neglect redshift effects and assume a homogeneous DMa density  $\rho_{\text{dm}} \approx 0.3 \text{ GeV/cm}^3$ . We select a set of  $N = 13$  pulsars with the smallest values of  $\text{DM}_{\text{obs}}/d$  and for which parallax measurements of the distance  $d$  are available [29]. We only choose pulsars located away from the galactic plane. This is to minimize the effect of the evacuation of DMa from the galactic plane for millicharged DMa with charge  $\epsilon \gtrsim 5.4 \times 10^{-22} \left( \frac{m_{\text{milli}}}{\text{eV}} \right)$  [16, 30]. Similarly, we build a second dataset of  $N_{\text{cluster}} = 13$  pulsars located in globular clusters within 8 kpc from the galactic center and off the disk, again with the smallest  $\text{DM}_{\text{obs}}/d$ . Distances of clusters can be determined by different methods [31] not relying on the DM, and their uncertainty is usually of a few percent. We therefore assign a conservative error of 10% to the value of  $d$  for the pulsars in this second dataset. Even if the effect of the galactic magnetic field on the density of millicharged DMa away from the galactic disk is not known, we do not expect DMa to be evacuated at high latitudes, and our analysis should provide realistic constraints.

For each pulsar we compute  $\text{DM}_{\text{astro}}^i \approx \langle n_e \rangle_i d_i$ , where  $\langle n_e \rangle_i$  is an average electron density along the line of sight obtained using the YMW16 model [32], while  $d_i$  is the pulsar distance obtained from parallax (for the first dataset) or from the location of the globular cluster (for the second dataset). In the former case, we assign  $\langle n_e \rangle_i$  a 20% error to take into account potential systematics in the electron density model. We perform a Monte-Carlo Markov chain analysis using the PYTHON ensemble sampler EMCEE [33] to explore the posterior distribution.

For our datasets,  $10^5$  samples are accumulated with 20 chains. The chains show good acceptance rate and convergence. The results are similar for the two datasets:

$$\frac{\epsilon}{m_{\text{milli}}} \lesssim \frac{4 \times 10^{-9}}{\text{eV}} \sqrt{\frac{0.3 \text{ GeV/cm}^3}{\rho_{\text{milli}}}} \text{ at 95\% C.L.} \quad (12)$$

which we compare to other existing bounds in Fig. 1. For completeness, we also show a similar (weaker) bound estimated from the dispersion of the fast radio burst FRB 121102 [34]. A more comprehensive analysis for FRBs will be presented elsewhere [10].

The mass range in Fig. 1 is limited on the left because the dispersion due to the plasma frequency is valid as long as the energy of the photon is larger than  $m_{\text{milli}}$ . For radio waves from pulsars,  $m_{\text{dm}} \gtrsim \omega \sim \text{GHz} \sim 10^{-6} \text{ eV}$ . Since the bound is more stringent for small masses, these constraints could improve if sub-GHz precision pulsar measurements become available, see e.g. Ref. [35]. Figure 1 shows that our bounds are competitive for masses below the Tremaine-Gunn bound on fermionic DMa,  $m_{\text{DMa}} \gtrsim \text{keV}$  [36]. Hence, they apply to scalar charged DMa or for models with a fraction of millicharged fermionic DMa (see Eq. (12)).

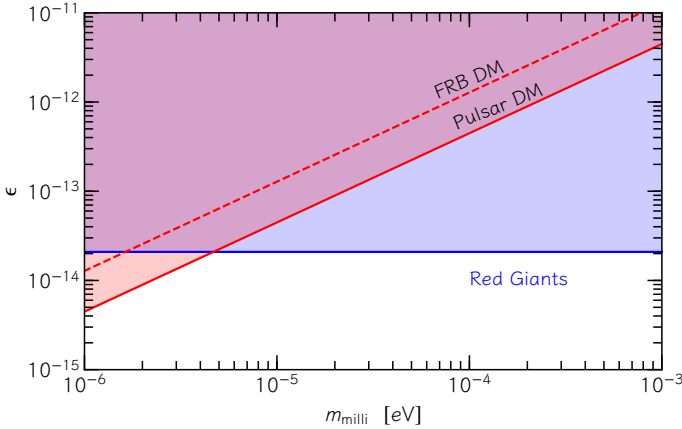


FIG. 1. Constraint on millicharged DMa in the  $\epsilon - m_{\text{milli}}$  space from pulsar (solid red line) and FRB 121102 (dashed red line) DM at 95% confidence level. Solid blue line indicates the bound from Red Giants [15]. We assume a homogeneous DMa density  $\rho_{\text{dm}} = \rho_{\text{milli}} \approx 0.3 \text{ GeV/cm}^3$ . The bound scales as  $\rho_{\text{milli}}^{-1/2}$  for fractional components.

**TOA constraints on ALPs.** In this case we neglect millicharged DMa and consider photon propagation in a magnetic field in the presence of an ALP-photon coupling. This computation does not depend on the DMa density, but only on the mixing. Therefore, we do not require that the ALPs are necessarily the DMa. For simplicity, we consider two regimes separately, namely  $m_a \gg \sqrt{2Bg\omega}$  and  $m_a \ll \sqrt{2Bg\omega}$ . In the former case we

get

$$v_{\pm}^{-1} = 1 + \frac{m_a^2}{2\omega^2} \mp \frac{m_a^2 + \omega_p^2}{8\omega^2} \eta^2 \pm \frac{3}{16} \frac{\omega_p^2}{\omega^2} \eta^4, \quad (13)$$

where now  $\omega_p$  is due to ordinary free electrons. Because  $\eta^2 \propto \omega^2$ , the  $\mathcal{O}(\eta^2)$  correction in the above dispersion relation gives a term which is independent of  $\omega$  and will therefore equally change the TOA at all frequencies. However, the  $\mathcal{O}(\eta^4)$  term gives a correction which scales as  $\omega^2$ . The corresponding delay in the TOA of the “+” polarization reads

$$\Delta t_{\text{axion}} = \nu^2 \int_0^d dl \frac{12\pi^2 B^4 g^4 \omega_p^2}{m_a^8}, \quad m_a \gg \sqrt{2Bg\omega}. \quad (14)$$

In the opposite regime,  $m_a \ll \sqrt{2Bg\omega}$ ,

$$v_{\pm}^{-1} = 1 + \frac{m_a^2 + \omega_p^2}{4\omega^2} \pm \frac{m_a^2 - 2\omega_p^2}{4\omega^2} \frac{1}{\eta}, \quad (15)$$

and the corresponding delay in the TOA scales as  $1/\omega^3$ ,

$$\Delta t_{\text{axion}} = \frac{1}{\nu^3} \int_0^d dl \frac{m_a^2(m_a^2 - 2\omega_p^2)}{64\pi^3 Bg}, \quad m_a \ll \sqrt{2Bg\omega}. \quad (16)$$

Thus, ALPs introduce a novel peculiar dependence of the TOA on the frequency which adds to the standard  $1/\nu^2$  behavior of Eq. (8),

$$\Delta t = 4.15 \text{ ms} \left( \frac{\text{DM}}{\nu^2} + \delta(\nu) \right), \quad (17)$$

where  $\delta(\nu) \propto \nu^2$  or  $\delta(\nu) \propto 1/\nu^3$  for  $m_a \gg \sqrt{2Bg\omega}$  or  $m_a \ll \sqrt{2Bg\omega}$ , respectively. Measurements of the frequency dependence of the TOA can therefore be used to put constraints on the ALP mass and coupling constant. This would require a precise sampling of the TOA as a function of the frequency, which will be soon available from wide-band observations [43, 44].

In order to estimate the projected bounds from this effect, we simulated the time delay in the bandwidth of observation for the aforementioned set of pulsars, using the corresponding values of  $\text{DM}_{\text{astro}}$  and their measurement errors as a proxy. We assumed ten measurements of the TOA at ten different frequencies in the range [1, 2] GHz, and then used the simulated data to constrain the coupling  $g$  for a range of ALP masses, using a maximum likelihood estimation performed with EMCEE. In the analysis we have set the magnetic field to the value  $B = 10^{-6} \text{ G}$  and used the YMW16 model for the electron density  $n_e$  [32]. These are conservative assumptions, since for an optimal source the magnetic field can be as high as  $B \sim 10^{-3} \text{ G}$  [45, 46] and  $n_e$  can be larger than the typical value  $n_e \approx 0.01 \text{ cm}^{-3}$  of our dataset. In Fig. 2 we show the projected constraints derived at 95% confidence level using the simulated TOA pulsar data. Our bounds extend to lower mass than the astrophysical constraints

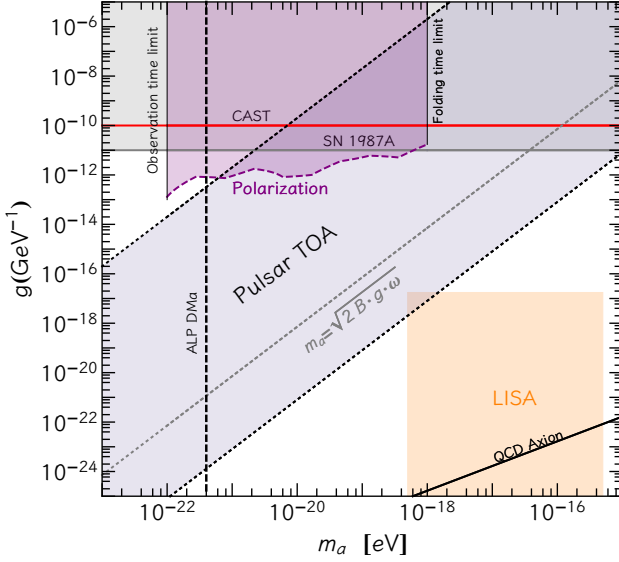


FIG. 2. Constraints for ALP DMA in the plane  $g - m_a$ . The shaded light-gray regions are projected constraints excluded at 95% confidence level by TOA pulsar data for the reference value  $B = 10^{-6}$  G. The dotted black lines correspond to the upper and lower bounds from the two regimes in Eq. 16 and Eq. 14, respectively, while the dotted gray line corresponds to the separatrix  $m_a = \sqrt{2B \cdot g \cdot \omega}$  for  $\nu = 1$  GHz. The dash-dotted purple line indicates instead the lower bound set by polarization measurements using real data. Finally, the darker gray band indicates the region excluded by CAST experiment [37] and by supernova cooling [38], whereas the orange area is the projected bound coming from gravitational-wave searches with LISA [39, 40], assuming a dense population of highly-spinning supermassive black holes and considering an upper bound on the ALP-photon coupling coming from quenching of the superradiance instability [41, 42].

on ALP DMA, namely  $m_a \sim 10^{-22}$  eV [47, 48] shown in Fig. 2 by a vertical dashed line.

**Polarization constraints on ALPs.** Due to their pseudo-scalar nature, ALPs also induce an oscillating variation of light polarization [49–53]. Parity-symmetry breaking leads to birefringence, i.e. different phase velocities for left- and right-handed modes, which in turn induces rotation of the linear polarization plane. In the presence of an ALP-DMA background with profile  $\vec{\phi}(t, \vec{x}) = \phi_0 \cos(m_a t - \vec{k}_\phi \cdot \vec{x})$ , and density  $\rho_{\text{dm}} = \frac{1}{2} m_a^2 \phi_0^2$ , the polarization angle of a photon propagating from time  $t$  to  $t + T$  reads [52]

$$\theta(t, T) \sim 1.4 \times 10^{-2} \sin(m_a t + \delta) \left( \frac{g}{10^{-12} \text{ GeV}^{-1}} \right) \times \begin{cases} \frac{10^{-22} \text{ eV}}{m_a}, & \mathcal{N} < 1 \\ \sqrt{\frac{10^{-22} \text{ eV}}{m_a}} \sqrt{\frac{v}{10^{-3}}} \sqrt{\frac{T}{400 \text{ pc}}}, & \mathcal{N} > 1 \end{cases}, \quad (18)$$

where  $\delta$  is a constant phase,  $\mathcal{N} = T/\lambda$  is number of crossed coherent patches,  $\lambda$  being the ALP de Broglie wavelength. The characteristic time scale for the axion

background oscillation is  $T_{\text{ALP}} \sim \frac{10^{-22} \text{ eV}}{m_a} \text{ yr}$ ; if one continuously observes the polarized light from the source during a time  $t_{\text{obs}} \gtrsim T_{\text{ALP}}$ , the observed variation of the polarization angle (18) may constrain the amplitude of the axion oscillations, i.e. the coupling  $g$  for a given mass  $m_a$ . Pulsars are observed for long periods and the polarization angle is measured to be almost constant with a precision of roughly one degree, that can be compared with Eq. (18). We use the polarization data from Ref. [54] and in particular PSR J0437–4715, which is the pulsar with the highest number of observations of the polarization angle, spanning a period of roughly four years. The ionospheric contribution to the polarization angle was subtracted using the program GETRM-IONO [55]. We performed a likelihood estimation of the coupling  $g$  for a set of fixed masses  $m_a$ . For each value of the mass, we marginalize over the unknown phase  $\delta$  in Eq. (18) in the interval  $[-\pi, \pi]$  and then obtained the 95% C.L. exclusion value for  $g$ , which is our reported constraint.

The excluded region in Fig. 2 spans roughly five orders of magnitude in the mass range, from  $m_a \sim 10^{-18}$  eV to  $m_a \sim 10^{-22}$  eV. The lower limit is set by the total observation time ( $\sim 4$  yr), whereas the upper limit is set by the folding time, that is 64 minutes for J0437–4715. As long as  $\mathcal{N} > 1$  in Eq. (18), the derived lower bounds scale as  $1/\sqrt{m_a}$  — with some modulation due to the fact that observations of the polarization angle for J0437–4715 are not homogeneous in time — and is stronger for smaller masses, i.e. longer observation time. The bound scales as  $\sim \rho_{\text{dm}}$ , so it can be competitive even if ALPs form only a small fraction of the DMA.

**Discussion.** Several DMA models introduce dispersion effects in the photon propagation. Although small, these effects accumulate for photons coming from astrophysical sources and can be constrained through precision measurements. The effect of millicharged DMA is degenerate with that of ordinary plasma and improving models for the local plasma distribution will help strengthening the constraints from DM. On the other hand, the effect of ALP-photon coupling is more striking and requires a careful analysis of the TOA as a function of the frequency. We argue that the TOA precision measurements are a promising diagnostics for indirect searches for DMA and we advocate the need of precision wide-band observations in this direction [43, 44]. In addition, in the upcoming era of the Square Kilometre Array, we will benefit from a much larger pulsar sample (possibly comprising sources near the galactic center, where the DMA density is higher than what assumed here), combined with a significantly improved timing precision [56–58]. The prospects of using radio waves in probing DMA are very promising in the near future.

For ALPs, their coupling to photons generates both a modified dispersion relation that affects the TOA of radio pulses and an oscillation of the polarization angle of photons in the ultra-light DMA case. Our results in Fig. 2

show that, for most values of the mass in the allowed range, the bounds from the photon polarization angle are less stringent than the projected ones obtained with the TOA. This suggests that upcoming wide-band observations can significantly improve the bounds on ultralight ALPs, in a regime which is currently poorly constrained.

We have considered propagation in a weak magnetic field,  $B \sim 10^{-6}$  G, for which QED vacuum polarization effects are negligible. However, our formalism can be easily extended to include such effects, and might be relevant for propagation in strongly magnetized regions. A discussion of this effect will appear elsewhere [10].

**Note:** While this work was close to completion, Ref. [59] appeared on the arXiv, estimating constraints on ALPs using the polarization angle of radio waves from pulsars similar to those derived in the last part of our work. Although our analysis is different, our bounds from real data are compatible with the estimations of Ref. [59].

**Acknowledgments.** We are grateful to Richard Brito for interesting discussion. AC acknowledge support from national grants FPA2014-57816-P, FPA2017-85985-P and the European projects H2020-MSCAITN-2015//674896-ELUSIVES and H2020-MSCA-RISE2015. PP acknowledge financial support provided under the European Union’s H2020 ERC, Starting Grant agreement no. DarkGRA-757480, and support from the Amaldi Research Center funded by the MIUR program “Dipartimento di Eccellenza” (CUP: B8I18001170001) and by the GWverse COST Action CA16104, “Black holes, gravitational waves and fundamental physics.” Research at Perimeter Institute is supported by the Government of Canada through Industry Canada and by the Province of Ontario through the Ministry of Research and Innovation. LS was partially supported by the National Science Foundation of China (11721303), and XDB23010200.

- 
- [1] A. Khmelnitsky and V. Rubakov, JCAP **1402**, 019 (2014), arXiv:1309.5888 [astro-ph.CO].
  - [2] N. K. Porayko and K. A. Postnov, Phys. Rev. **D90**, 062008 (2014), arXiv:1408.4670 [astro-ph.CO].
  - [3] P. Pani, Phys. Rev. **D92**, 123530 (2015), arXiv:1512.01236 [astro-ph.HE].
  - [4] H. A. Clark, G. F. Lewis, and P. Scott, Mon. Not. Roy. Astron. Soc. **456**, 1394 (2016), [Erratum: Mon. Not. Roy. Astron. Soc. 464, no. 2, 2468 (2017)], arXiv:1509.02938 [astro-ph.CO].
  - [5] D. Blas, D. L. Nacir, and S. Sibiryakov, Phys. Rev. Lett. **118**, 261102 (2017), arXiv:1612.06789 [hep-ph].
  - [6] K. Schutz and A. Liu, Phys. Rev. **D95**, 023002 (2017), arXiv:1610.04234 [astro-ph.CO].
  - [7] I. De Martino, T. Broadhurst, S. H. Henry Tye, T. Chiueh, H.-Y. Schive, and R. Lazkoz, Phys. Rev. Lett. **119**, 221103 (2017), arXiv:1705.04367 [astro-ph.CO].
  - [8] A. Caputo, J. Zavala, and D. Blas, Phys. Dark Univ. **19**, 1 (2018), arXiv:1709.03991 [astro-ph.HE].
  - [9] J. A. Dror, H. Ramani, T. Trickle, and K. M. Zurek, (2019), arXiv:1901.04490 [astro-ph.CO].
  - [10] D. Blas, A. Caputo, M. Frías, P. Pani, L. Sberna, L. Shao, and W. Yan, “Probing dark matter with pulsar timing,” (in preparation).
  - [11] A. De Rujula, S. L. Glashow, and U. Sarid, Nucl. Phys. **B333**, 173 (1990).
  - [12] M. L. Perl and E. R. Lee, Am. J. Phys. **65**, 698 (1997).
  - [13] B. Holdom, Phys. Lett. **B166**, 196 (1986).
  - [14] K. Sigurdson, M. Doran, A. Kurylov, R. R. Caldwell, and M. Kamionkowski, Phys. Rev. **D70**, 083501 (2004), [Erratum: Phys. Rev. D73, 089903 (2006)], arXiv:astro-ph/0406355 [astro-ph].
  - [15] S. Davidson, S. Hannestad, and G. Raffelt, JHEP **05**, 003 (2000), arXiv:hep-ph/0001179 [hep-ph].
  - [16] S. D. McDermott, H.-B. Yu, and K. M. Zurek, Phys. Rev. **D83**, 063509 (2011), arXiv:1011.2907 [hep-ph].
  - [17] A. Berlin, N. Blinov, G. Krnjaic, P. Schuster, and N. Toro, (2018), arXiv:1807.01730 [hep-ph].
  - [18] R. D. Peccei and H. R. Quinn, Phys. Rev. Lett. **38**, 1440 (1977), [,328(1977)].
  - [19] S. Weinberg, Phys. Rev. **140**, B516 (1965).
  - [20] J. Preskill, M. B. Wise, and F. Wilczek, Phys. Lett. **B120**, 127 (1983), [,URL(1982)].
  - [21] G. Raffelt and L. Stodolsky, Phys. Rev. **D37**, 1237 (1988).
  - [22] A. Dupays, C. Rizzo, M. Roncadelli, and G. F. Bignami, Phys. Rev. Lett. **95**, 211302 (2005), arXiv:astro-ph/0510324 [astro-ph].
  - [23] S. L. Adler, Annals Phys. **67**, 599 (1971).
  - [24] M. Gell-Mann, M. L. Goldberger, and W. E. Thirring, Phys. Rev. **95**, 1612 (1954), [,493(1954)].
  - [25] M. L. Goldberger and K. M. Watson, *Collision Theory* (Wiley, New York, 1964).
  - [26] D. C. Latimer, Phys. Rev. **D88**, 063517 (2013), arXiv:1308.1112 [hep-ph].
  - [27] S. Gardner and D. C. Latimer, Phys. Rev. **D82**, 063506 (2010), arXiv:0904.1612 [hep-ph].
  - [28] L. Shao and B. Zhang, Phys. Rev. **D95**, 123010 (2017), arXiv:1705.01278 [hep-ph].
  - [29] R. N. Manchester, G. B. Hobbs, A. Teoh, and M. Hobbs, Astronomical Journal **129**, 1993 (2005), astro-ph/0412641.
  - [30] L. Chuzhoy and E. W. Kolb, JCAP **0907**, 014 (2009), arXiv:0809.0436 [astro-ph].
  - [31] L. M. Krauss and B. Chaboyer, Science **299**, 65 (2003), <http://science.sciencemag.org/content/299/5603/65.full.pdf>.
  - [32] J. M. Yao, R. N. Manchester, and N. Wang, The Astrophysical Journal **835** (2016), 10.3847/1538-4357/835/1/29.
  - [33] D. Foreman-Mackey, D. W. Hogg, D. Lang, and J. Goodman, Publ. Astron. Soc. Pac. **125**, 306 (2013), arXiv:1202.3665 [astro-ph.IM].
  - [34] S. Chatterjee *et al.*, Nature **541**, 58 (2017), arXiv:1701.01098 [astro-ph.HE].
  - [35] M. Pilia *et al.*, Astron. Astrophys. **586**, A92 (2016), arXiv:1509.06396 [astro-ph.HE].
  - [36] S. Tremaine and J. E. Gunn, Phys. Rev. Lett. **42**, 407 (1979), [,66(1979)].
  - [37] V. Anastassopoulos *et al.* (CAST), Nature Phys. **13**, 584 (2017), arXiv:1705.02290 [hep-ex].
  - [38] A. Payez, C. Evoli, T. Fischer, M. Giannotti, A. Mirizzi, and A. Ringwald, JCAP **1502**, 006 (2015),

- arXiv:1410.3747 [astro-ph.HE].
- [39] R. Brito, S. Ghosh, E. Barausse, E. Berti, V. Cardoso, I. Dvorkin, A. Klein, and P. Pani, Phys. Rev. **D96**, 064050 (2017), arXiv:1706.06311 [gr-qc].
  - [40] R. Brito, S. Ghosh, E. Barausse, E. Berti, V. Cardoso, I. Dvorkin, A. Klein, and P. Pani, Phys. Rev. Lett. **119**, 131101 (2017), arXiv:1706.05097 [gr-qc].
  - [41] A. Arvanitaki, M. Baryakhtar, and X. Huang, Phys. Rev. **D91**, 084011 (2015), arXiv:1411.2263 [hep-ph].
  - [42] T. Ikeda, R. Brito, and V. Cardoso, (2018), arXiv:1811.04950 [gr-qc].
  - [43] T. E. Hassall, B. W. Stappers, J. W. T. Hessels, M. Kramer, A. Alexov, *et al.*, A&A **543**, A66 (2012), arXiv:1204.3864 [astro-ph.HE].
  - [44] T. T. Pennucci, P. B. Demorest, and S. M. Ransom, Astrophysical Journal **790**, 93 (2014), arXiv:1402.1672 [astro-ph.IM].
  - [45] M. Haverkorn, in *Magnetic Fields in Diffuse Media*, Astrophysics and Space Science Library, Vol. 407, edited by A. Lazarian, E. M. de Gouveia Dal Pino, and C. Melioli (2015) p. 483, arXiv:1406.0283 [astro-ph.GA].
  - [46] J. Han, Annual Review of Astronomy and Astrophysics **55**, 111 (2017), <https://doi.org/10.1146/annurev-astro-091916-055221>.
  - [47] T. Kobayashi, R. Murgia, A. De Simone, V. Irsi, and M. Viel, Phys. Rev. **D96**, 123514 (2017), arXiv:1708.00015 [astro-ph.CO].
  - [48] N. Bar, D. Blas, K. Blum, and S. Sibiryakov, Phys. Rev. **D98**, 083027 (2018), arXiv:1805.00122 [astro-ph.CO].
  - [49] D. Harari and P. Sikivie, Phys. Lett. **B289**, 67 (1992).
  - [50] M. M. Ivanov, Y. Y. Kovalev, M. L. Lister, A. G. Panin, A. B. Pushkarev, T. Savolainen, and S. V. Troitsky, (2018), arXiv:1811.10997 [astro-ph.CO].
  - [51] G. Sigl and P. Trivedi, (2018), arXiv:1811.07873 [astro-ph.CO].
  - [52] T. Fujita, R. Tazaki, and K. Toma, (2018), arXiv:1811.03525 [astro-ph.CO].
  - [53] A. D. Plascencia and A. Urbano, JCAP **1804**, 059 (2018), arXiv:1711.08298 [gr-qc].
  - [54] W. Yan *et al.*, Astrophys. Space Sci. **335**, 485 (2011), arXiv:1105.4213 [astro-ph.SR].
  - [55] J. L. Han, R. N. Manchester, A. G. Lyne, G. J. Qiao, and W. van Straten, Astrophys. J. **642**, 868 (2006), arXiv:astro-ph/0601357 [astro-ph].
  - [56] M. Kramer and B. Stappers, in *Advancing Astrophysics with the Square Kilometre Array*, Vol. AASKA14 (Proceedings of Science, 2015) p. 036.
  - [57] L. Shao *et al.*, in *Advancing Astrophysics with the Square Kilometre Array*, Vol. AASKA14 (Proceedings of Science, 2015) p. 042, arXiv:1501.00058 [astro-ph.HE].
  - [58] P. Bull *et al.*, (2018), arXiv:1810.02680 [astro-ph.CO].
  - [59] T. Liu, G. Smoot, and Y. Zhao, (2019), arXiv:1901.10981 [astro-ph.CO].